SCIENTIFIC REPORTS

OPEN

SUBJECT AREAS:
CELLULAR MICROBIOLOGY
FUNGAL BIOLOGY

Received
23 June 2014

Accepted
4 August 2014

Published
2 September 2014

Correspondence and requests for materials should be addressed to M.H.V. (mhv@cbiot.ufrgs.br) or M.L.R. (marciolr@cdts.fiocruz.br)

* These authors contributed equally to this work.

The vacuolar-sorting protein Snf7 is required for export of virulence determinants in members of the *Cryptococcus neoformans* complex.

Rodrigo M. da C. Godinho[1]*, Juliana Crestani[2]*, Lívia Kmetzsch[2], Glauber de S. Araujo[3,4], Susana Frases[3,4], Charley C. Staats[2], Augusto Schrank[2,5], Marilene H. Vainstein[2,5] & Marcio L. Rodrigues[1,6]

[1]Instituto de Microbiologia Paulo de Góes, Universidade Federal do Rio de Janeiro, 21941-902, Rio de Janeiro, Brazil, [2]Centro de Biotecnologia, Universidade Federal do Rio Grande do Sul, Caixa Postal 15005, Porto Alegre, RS 91501-970, Brazil, [3]Laboratório de Ultraestrutura Celular Hertha Meyer, Instituto de Biofisica Carlos Chagas Filho, Universidade Federal do Rio de Janeiro, Brazil, [4]Laboratório de Biologia, Instituto Nacional de Metrologia, Normalização e Qualidade Industrial (INMETRO), Rio de Janeiro, Brazil, [5]Departamento de Biologia Molecular e Biotecnologia, Universidade Federal do Rio Grande do Sul, Porto Alegre, RS 91501-970, Brazil, [6]Fundação Oswaldo Cruz - Fiocruz, Centro de Desenvolvimento Tecnológico em Saúde (CDTS), Rio de Janeiro, Brazil.

Fungal pathogenesis requires a number of extracellularly released virulence factors. Recent studies demonstrating that most fungal extracellular molecules lack secretory tags suggest that unconventional secretion mechanisms and fungal virulence are strictly connected. Proteins of the endosomal sorting complex required for transport (ESCRT) have been recently associated with polysaccharide export in the yeast-like human pathogen *Cryptococcus neoformans*. Snf7 is a key ESCRT operator required for unconventional secretion in Eukaryotes. In this study we generated *snf7*Δ mutant strains of *C. neoformans* and its sibling species *C. gattii*. Lack of Snf7 resulted in important alterations in polysaccharide secretion, capsular formation and pigmentation. This phenotype culminated with loss of virulence in an intranasal model of murine infection in both species. Our data support the notion that Snf7 expression regulates virulence in *C. neoformans* and *C. gattii* by ablating polysaccharide and melanin traffic. These results are in agreement with the observation that unconventional secretion is essential for cryptococcal pathogenesis and strongly suggest the occurrence of still obscure mechanisms of exportation of non-protein molecules in Eukaryotes.

Cryptococcosis is the leading cause of human deaths related to fungal infections in Africa[1]. This disease is caused by the yeast-like pathogens *Cryptococcus neoformans* and *C. gattii*. The former is an opportunistic fungal pathogen that causes highly lethal meningitis in immunocompromised individuals[2]. *C. gattii*, on the other hand, can infect both immunocompromised and immunocompetent individuals[3].

The progress of cryptococcal disease relies on several extracellular virulence factors[4,5], implying that secretion is fundamental for cryptococcal pathogenesis. Eukaryotic molecules are exported through different cellular pathways, including conventional and unconventional secretory routes[6,7]. Conventionally secreted proteins follow the classical endoplasmic reticulum (ER)/Golgi-dependent secretory pathway[7]. Protein secretion through conventional mechanisms is dependent of an N-terminus-linked signal peptide, which is responsible for translocation of polypeptides into the lumen of the ER[7]. Proteins that lack a typical signal peptide are transported independently of this classical ER-Golgi route and engage the so-called unconventional secretion mechanisms[6].

Most of the pathogenic determinants of *C. neoformans* lack secretory tags, supporting the notion that unconventional pathways of secretion are required for cryptococcal virulence[8]. *C. neoformans* and *C. gattii* export massive amounts of polysaccharides to the extracellular milieu[9,10]. Polysaccharide export is required for capsule formation, which is essential for the survival of cryptococci in host tissues[11–14]. The main component of the polysaccharide capsule is glucuronoxylomannan (GXM). GXM is co-transported to the extracellular space with other virulence factors inside vesicles that traverse the cell wall[15–17]. Although the morphological aspects of these vesicles suggest that they are similar to mammalian exosomes, their cellular origin remains undetermined (reviewed by Oliveira and colleagues[18]).

The eukaryotic sucrose non-fermenting protein 7 (Snf7) is a key operator in the endosomal sorting complex required for transport (ESCRT)-III[19,20]. This molecular complex, in association with other ESCRT components, is involved in multivesicular body (MVB) formation and cargo. MVB formation requires Snf7 oligomerization into a membrane-associated filament, which is nucleated by its association with the vacuolar protein sorting regulator Vps20[21]. MVBs, which derive from late endosomes, can be directed for fusion with the plasma membrane, resulting in extracellular release of their luminal vesicles, the so-called exosomes[22,23]. The ESCRT machinery has also been implicated in environmental pH sensing and adaptation in various fungal species through mechanisms that require the RIM101 pathway, a signaling mechanism necessary for the regulation of alkaline environment-related genes[24,25]. Recently, the RIM101-mediated stress response has been demonstrated to be up regulated during human meningitis caused by *C. neoformans*[26]. The supposition that MVBs are associated with the export of virulence factors in *C. neoformans*[17] and the fact that adaptation to alkaline pHs is required for fungal survival in both alveolar spaces and the bloodstream[27] suggests that *SNF7* is involved in cryptococcal pathogenicity.

In this work we generated *C. neoformans* and *C. gattii snf7Δ* mutant strains and characterized their biological and pathogenic properties. Lack of Snf7 affected key virulence determinants in both *C. neoformans* and *C. gattii*. This phenotype culminated with loss of virulence in an intranasal model of murine infection in both species. These results strongly support the hypothesis that unconventional secretion pathways are essential for the pathogenesis of *C. neoformans* and *C. gattii*.

Results

Snf7-related sequences in *C. neoformans* and *C. gattii*. A database search of the *C. gattii* genome (http://www.broadinstitute.org/annotation/genome/cryptococcus_neoformans_b/MultiHome.html-August 5, 2009, strain R265) revealed that the *SNF7* (accession number CNBG_3856) coding region comprises 1,087 bp, includes five introns, and encodes a protein of 221 amino acids. A similar search in the *C. neoformans* genome (http://www.broadinstitute.org/annotation/genome/cryptococcus_neoformans/MultiHome.html) identified the putative *SNF7* sequence (accession number CNAG_01583.2) based on the similarity to the corresponding *C. gattii* sequence (accession number CNBG_3856). The *C. neoformans SNF7* ortholog is 1,413 bp long, contains five introns, and also encodes a putative 221 amino-acid protein. Phylogenetic analysis of Snf7 was performed with orthologues from distinct eukaryotic organisms (Figure 1A). The putative sequence of the *C. gattii* protein was highly similar to its *C. neoformans* counterpart (98% identity) and both display similarities to plant proteins (*A. thaliana* ~35% identity; *O. sativa* ~24% identity). In comparison to other fungi, the Snf7 sequences of both species studied here showed 45% identity with the *S. cerevisiae* protein and 43% identity with a *C. albicans* homologue.

Disruption and complementation of *SNF7* genes in both *C. neoformans* and *C. gattii*. To analyze the functions of *SNF7*, we generated *snf7Δ* disruption mutants in the backgrounds of the standard strains H99 (serotype A isolate of *C. neoformans*) and R265 (serotype B isolate of *C. gattii*). These mutant strains were called CN-*snf7Δ* and CG-*snf7Δ*, respectively. To ensure that the eventual phenotypes observed in the mutant strains were due to the knockout of the *SNF7* gene, we constructed the complemented strains (CN-*snf7Δ*::*SNF7* for *C. neoformans* and CG-*snf7Δ*::*SNF7* for *C. gattii*) by integrating a wild-type copy of the *SNF7* gene into the genome of the mutant strains. Deletion and complementation of *SNF7* in both species were confirmed by Southern blot analysis (Figure 1B) and RT-PCR (Figure 1C).

Growth rates of the *snf7Δ* mutants under different conditions. We first evaluated whether the growth rates of the *snf7Δ* strains varied under different conditions. *C. neoformans* and *C. gattii* mutant strains showed normal growth at both 30 and 37°C, in comparison to parental and reconstituted strains (Figure 2A). Since copper acquisition is important for *C. neoformans* melanization and capsule formation[28,29] we also evaluated the ability of the *snf7Δ* mutants to grow under copper deprivation conditions. Once again, the mutants showed normal growth rates, in comparison to WT and complemented cells (Figure 2B).

The ESCRT machinery, including Snf7, plays a central role in resistance to higher pHs and tolerance to ionic lithium[30–32]. Therefore, we analyzed the ability of the *snf7Δ* mutants to survive under these conditions. Analysis of fungal growth in pHs ranging from 7 to 9 suggested lower growth rates of both CN-*snf7Δ* and CG-*snf7Δ* in pHs above 7.5, in comparison to parental and reconstituted cells (Figure 2C; $p < 0.05$ for all comparisons between cells expressing Snf7 and *snf7Δ* strains). A similar result was obtained when the *C. neoformans* and *C. gattii* strains were cultivated in the presence of 150 mM $LiCl_2$ (Figure 2D). The phenotypes described above in *C. neoformans* and other fungal species are related to the interaction between Snf7 and molecules belonging to the RIM101 pathway (Figure 3A), which includes Rim101p and Rim20p[30,33–35]. Therefore, to support the notion that the phenotypes we observed were linked to defects in Rim101p activation via interaction with Snf7/Rim20p we assessed the expression of *RIM101* and *RIM20*. We observed that although the mRNA levels of *RIM20* remained the same for all strains, the expression of *RIM101* was significantly lower in both *snf7Δ* mutants (Figure 3B and C). This observation is in agreement with a lower activation of RIM101p due to lack of Snf7.

***SNF7* disruption alters pigmentation but not urease and phospholipase activities.** Extracellularly released enzymes and exported pigments are fundamental for cryptococcal pathogenesis[5,17,36–39]. Therefore, we analyzed whether *SNF7* disruption would impact melanization and the extracellular activities of urease and phospholipase. Pigmentation was evaluated visually after growth of *C. neoformans* and *C. gattii* on both Niger seed and L-DOPA-containing solid media (Figure 4A). Under both conditions, the CN-*snf7Δ* mutant strain was similar to parental (WT) and complemented (reconstituted) strains in its ability to melanize at 30°C. However, when cultivated at 37°C, the mutant CN-*snf7Δ* showed reduced pigmentation. Differently, the CG-*snf7Δ* mutant showed subtle melanization defects when cultivated on L-DOPA agar at 30°C. At 37°C, the pigmentation defects were more evident. On Niger seed agar, *SNF7* deletion in *C. gattii* affected pigmentation at 30°C, but not at 37°C. These results revealed an unexpected interspecies diversity in the relationship between Snf7 and pigmentation.

Crude phospholipase activity was also assessed in the *SNF7* disruption model. Although the rate of phospholipid hydrolysis showed some tendency to be higher in the CN-*snf7Δ* mutant, there were no statistical differences between any of the *C. neoformans* strains (Figure 4B). The *C. gattii snf7* mutant showed levels of phospholipase activity that tended to be lower than those observed for parental and complemented strains (Figure 4B). Urease activity was similar in all strains analyzed in this study (Figure 4C).

Lack of Snf7 severely impairs GXM secretion and capsule formation. GXM secretion and capsule enlargement are essential for cryptococcal pathogenesis (reviewed in[40]). Since it has been suggested that GXM is exported by unconventional secretion mechanisms (reviewed elsewhere[9,15,41]), we evaluated whether *SNF7* deletion affects capsule size and extracellular polysaccharide secretion.

Quantification of secreted GXM in all strains by ELISA revealed that deletion of *SNF7* nearly extinguished polysaccharide export in both *C. neoformans* and *C. gattii* (Figure 5A). Morphological analysis of the capsule by India ink counterstaining, immunostaining of GXM

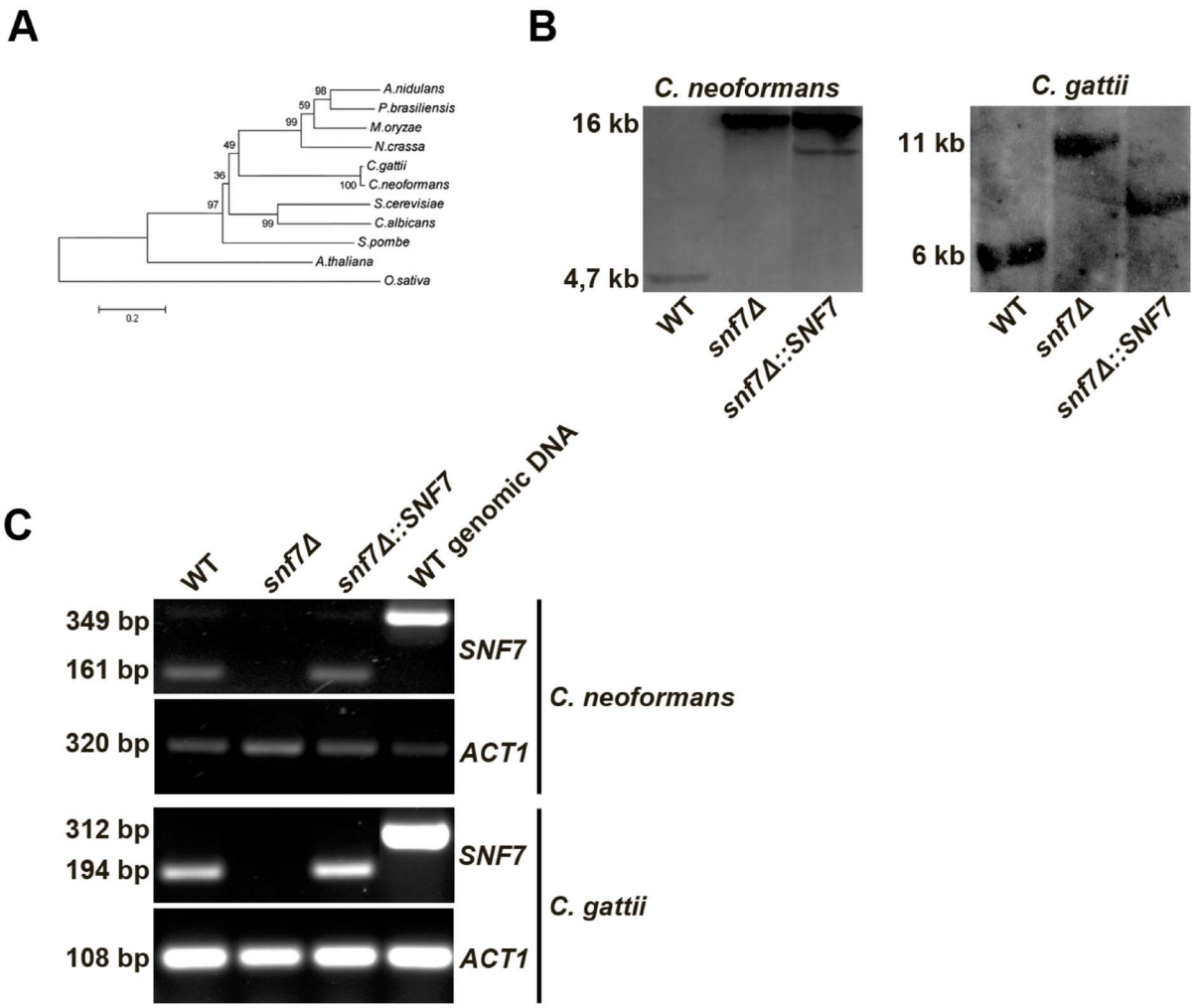

Figure 1 | Analysis of cryptococcal *SNF7*. (A). Phylogenetic analysis was performed by applying the neighbor-joining method with Snf7 amino acid sequences from distinct organisms as follows: *S. cerevisiae*, *C. albicans*, *A. nidulans*, *P. brasiliensis*, *S. pombe*, *N. crassa*, *M. oryzae*, *A. thaliana*, *O. sativa*, *C. neoformans* and *C. gattii*. The bar marker indicates the genetic distance, which is proportional to the number of amino acid substitutions. Bootstrap values obtained with 1,000 re-samplings are displayed at the nodes. (B). Analysis of *SNF7* disruption in *C. neoformans* and *C. gattii* by Southern blot. Genomic DNA (10 μg) from WT, *snf7Δ* and *snf7Δ*::*SNF7* strains were digested with the XbaI restriction enzyme. The 3′ gene flank was used as probe in Southern hybridization. (C). For RT-PCR, cDNA from *C. neoformans* and *C. gattii* (WT, *snf7Δ* and *snf7Δ*::*SNF7* strains) were used as template and genomic DNA of both fungi (WT cells) was used as positive control. Actin gene (*ACT1*) was used as reference gene for normalization of RT-PCR.

and scanning electron microscopy revealed a clear reduction in capsular dimensions in the *snf7Δ* mutants (Figure 5B), implying defects in capsular assembly. Determination of the capsule/cell diameter ratio confirmed a significant reduction ($p < 0.0001$) in capsular dimensions in both CN-*snf7Δ* and CG-*snf7Δ* cells (Figure 5C).

***snf7Δ* mutants are avirulent in a murine infection model.** The involvement of Snf7 in melanization, polysaccharide secretion and capsule assembly was in agreement with the possibility that *SNF7* deletion could affect pathogenesis. To address this question, mice were infected intranasally with each strain used in this work for mortality assessment. The totality of animals infected with wild type and CN-*snf7Δ*::*SNF7* reconstituted strains died by day 14 post infection (Figure 6A). Infection of mice with the CN-*snf7Δ* strain, however, resulted in nearly 63% survival at day 40-post infection, when animals were sacrificed. Animals infected with the *C. gattii snf7Δ* mutant had a survival rate of 87.5% by day 40 (Figure 6B). Mice infected with parental and complemented strains of *C. gattii* died by days 18 and 29, respectively. Statistical analysis (Mantel-Cox test) confirmed that *C. neoformans* ($p = 0.0065$) and *C. gattii* ($p = 0.0008$) cells lacking Snf7 were less efficient than parental and complemented strains in killing mice.

To assess GXM secretion in vivo, mice were infected with *C. neoformans* for determination of fungal loads and polysaccharide concentration in lung tissues (Figure 6C). In pulmonary samples from infected mice with the CN-*snf7Δ* mutant, the concentration of extracellular GXM was nearly half the values obtained when mice were infected with parental cells ($p = 0.0017$). Fungal loads were also greatly reduced when animals were infected with the CN-*snf7Δ* mutant, in comparison to animals infected with the wild type strain ($p < 0.0001$).

Discussion

Secretory activity is mandatory for cryptococcal pathogenesis. The vast majority of the well-characterized molecular determinants of cryptococci are extracellular, including GXM, urease and phospholipase B[17,37,42–44]. In addition, *C. neoformans* melanin, which is also fundamental for virulence, is exported to the cell surface by vesicle-dependent secretory mechanisms[17,45]. Except for phospholipase B, all the above-mentioned virulence factors lack the leader peptide

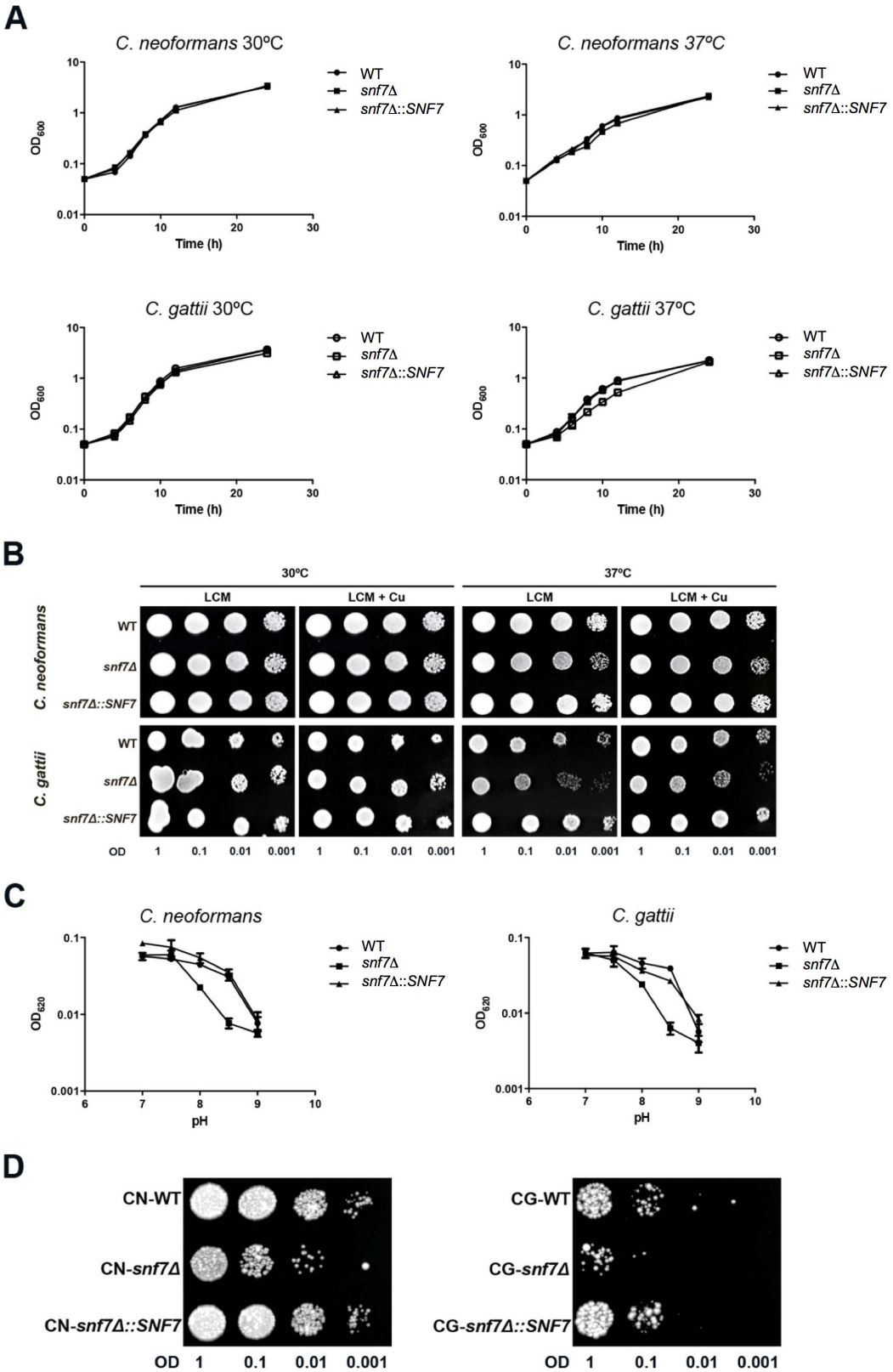

Figure 2 | Effects of *SNF7* disruption on fungal growth under different conditions. (A). Wild type (WT), mutant (*snf7Δ*) and complemented (*snf7Δ::SNF7*) strains of *C. neoformans* and *C. gattii* were grown in YPD broth with shaking at 30°C or 37°C. Growth measurements (OD_{600}) were performed at 4 h, 6 h, 8 h, 10 h, 12 h and 24 h. (B). Ten-fold serial dilutions of all strains were plated on LCM + Cu and LCM agar plates. The plates were incubated for 2 days at 30°C or 37°C. Fungal growth in LCM + Cu represented the control condition. (C). Growth rates of WT, mutant and complemented strains at pHs 7, 7.5, 8, 8.5 and 9. (D). Growth of WT, *snf7Δ* and *snf7Δ::SNF7* strains on YPD agar plates supplemented with 150 mM $LiCl_2$. Experiments were performed in triplicate and representative examples are shown.

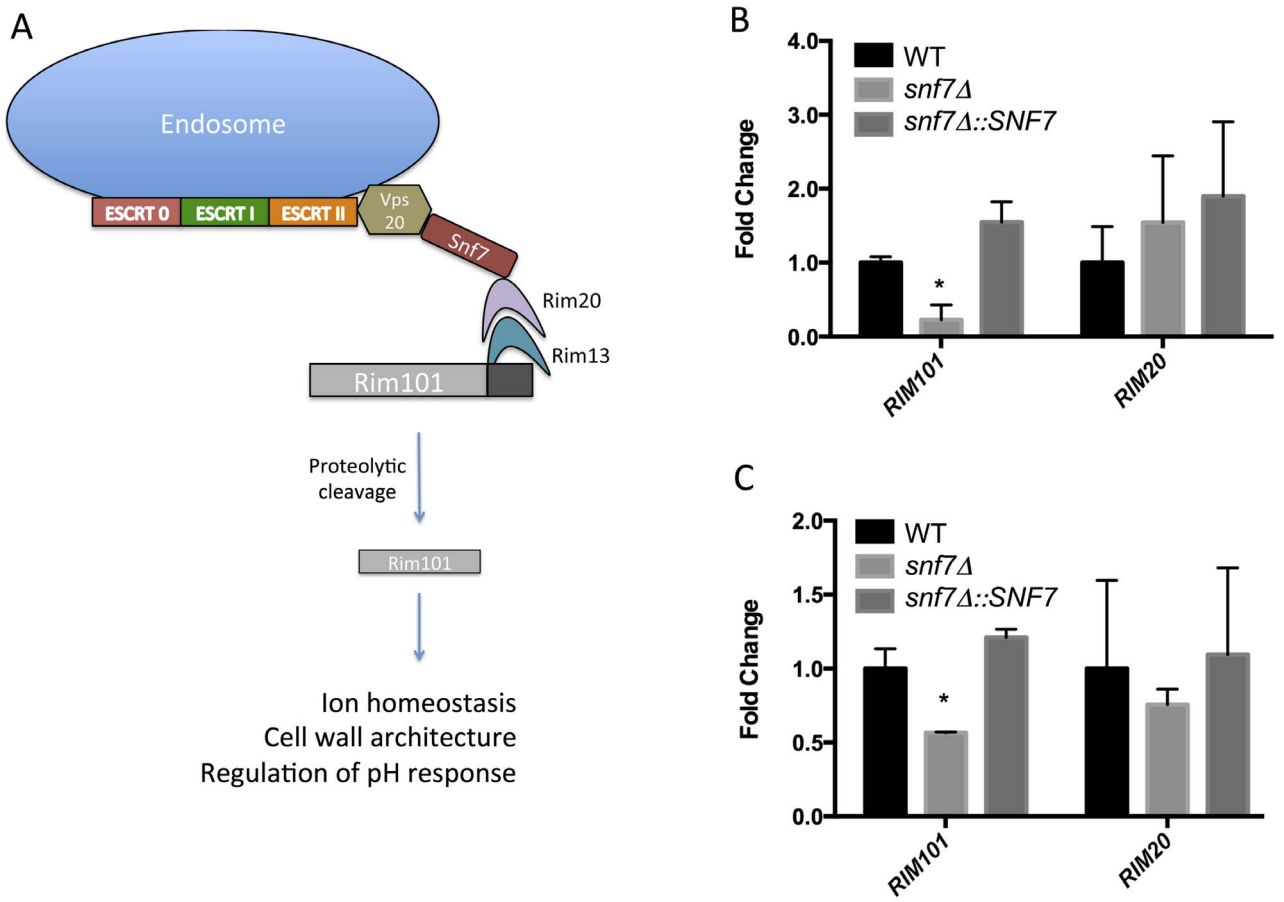

Figure 3 | ***SNF7* disruption affects the expression of *RIM101*.** (A). Conceptual basis for the analysis of Rim101 and Rim20 expression in *C. neoformans* and *C. gattii* strains. Rim101 activation depends on the recruitment of ESCRTI, ESCRTII and ESCRTIII components (Vps20 and Snf7) to the cytoplasmic face of the endosomal membrane. The Snf7 and Rim20/Rim13 protein complex interacts with the Rim101 precursor, which is further cleaved to release the active form of Rim101. This process results in the regulation of cryptococcal genes playing key roles in a number of cellular events. Adapted from Selvig and Alspaugh[87]. Expression levels of *RIM101* and *RIM20* were assessed in wild-type (WT), mutant (*snf7*) and complemented (*snf7*::*SNF7*) strains of *C. neoformans* (B) and *C. gattii* (C). The expression levels were normalized to the wild-type using the $2^{-\Delta\Delta Ct}$ [88].The experiments were performed with two biological samples, and each cDNA sample was analyzed in triplicate with each primer pair. (*, $p < 0.05$ in comparison with WT and complemented cells).

required for conventional secretion[46]. This observation and the recent notion that most fungal extracellular molecules lack secretory tags[17] strongly suggest that unconventional secretion mechanisms and fungal virulence are strictly connected. Due to high efficacy of both *C. neoformans* and *C. gattii* in exporting massive amounts of polysaccharides, we used this model to investigate connections between unconventional export of molecules and fungal pathogenesis.

The ESCRT machinery participates in MVB formation (reviewed in[23,47]), which is required for exosome release to the extracellular space. Snf7, one of the components of the ESCRTIII protein complex, is responsible for the genesis of intraluminal vesicles of MVBs[47]. Therefore, considering that fungal cells might use exosome-like vesicles for the transfer of intracellularly synthesized polysaccharides to the extracellular milieu[17], it seems reasonable to suppose that Snf7 is required for unconventional export of GXM in fungal cells. This hypothesis is supported by the fact that *C. neoformans sec* mutants, which have defects in post-Golgi, conventional secretory mechanisms, have normal capsules[48,49]. On the other hand, *C. neoformans* ESCRT-I mutants lacking expression of Vps23 manifested defective capsule formation and reduced virulence in a mouse model of cryptococcosis[50].

Most of the studies on secretory mechanisms in eukaryotic cells were focused on protein trafficking[17,48,51–55]. The mechanism for export of molecules of a non-protein nature, including pigments and polysaccharides, are poorly known. In mammalian cells, MVBs have been correlated with the initial biogenesis of melanosomes[56], implying connections between unconventional secretion and pigment traffic. In plant cells, endomembranes participate in polysaccharide traffic[57], but the identity of the components necessary for the transport of cell wall enzymes and polysaccharides is not known. In this study, deletion of *SNF7* resulted in reduced efficacies of pigmentation, GXM secretion and capsule formation in *C. neoformans* and *C. gattii*. These observations suggest that MVB formation and unconventional secretion mechanisms participate directly in the export of surface and/or extracellular molecules of non-protein nature. Although this hypothesis still needs experimental confirmation, it agrees with the observation that in *C. neoformans* Golgi reassembly and stacking protein (GRASP) and the Apt1 flippase, which are both unconventional secretion regulators, were required for polysaccharide, but not protein export[58–60].

Melanin is essential for cryptococcal virulence[61]. In our study, the effects of *SNF7* deletion on melanin formation varied depending on the species analyzed, temperature of growth and source of substrates for pigment synthesis. This observation efficiently illustrates the physiological diversity between the sibling species *C. neoformans* and *C. gattii*, which is likely linked to their well-known differences in pathogenic potential[3]. These results also exemplify the functional diversity of Snf7 in eukaryotes. In our model, fungal growth was only

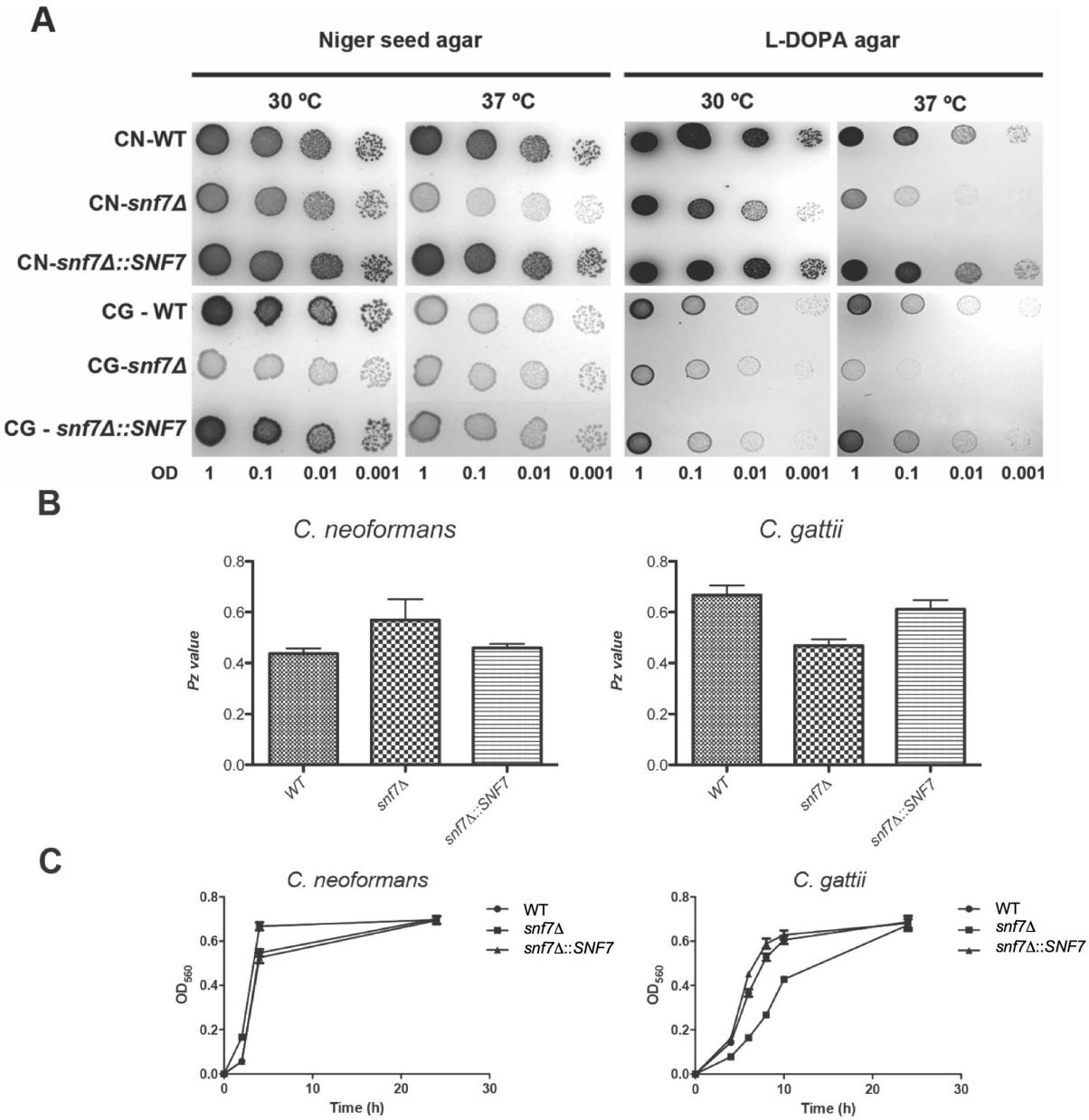

Figure 4 | Disruption of *SNF7* affects pigmentation but not extracellular enzyme activity. (A). Fungal cells were grown on Niger seed agar and L-DOPA plates to evaluate melanin production by wild-type (WT), mutant (*snf7Δ*) and complemented (*snf7Δ::SNF7*) strains of *C. neoformans* and *C. gattii*. The cultures were incubated at 30°C and 37°C and monitored for 2 (Niger), 3 (L-DOPA 30°C) or 4 (L-DOPA 37°C) days of cultivation. (B). Phospholipase activity in egg yolk agar. All strains were inoculated on plates containing egg yolk agar and incubated at 30°C for 4 days, and *Pz* values were then determined. (C). Urease activity levels of WT, *snf7Δ*, *snf7Δ::SNF7* cells. Fungal cells were incubated in urea broth with shaking (200 rpm) at 37°C for 24 hours for colorimetric determination. Statistical differences were not observed when parental, mutant and complemented strains were compared.

slightly affected in mutants cultivated at 37°C, but a previous study with *S. cerevisiae* lacking Snf7 demonstrated a clear correlation between carbon source and temperature-sensitive growth[62], suggesting an important metabolic variation that is affected by both nutrient availability and temperature of growth. The mechanisms explaining the differential ability of *C. neoformans* and *C. gattii* Snf7 mutants to produce pigments at different temperatures in the presence of distinct melanization substrates are still unknown, but our results and the seminal observations in the *S. cerevisiae* model[62] clearly support the notion that the physiological functions of Snf7 are regulated at multiple levels and result in variable fungal phenotypes. It is noteworthy that the enzymatic activity required for melanization can be also influenced by pH. Due to the putative roles of Snf7 in pH sensing[21,30], we cannot rule out the hypothesis that defective melanin formation resulted from altered laccase activity in the two species analyzed in our study.

SNF7 deletion also interfered with tolerance to alkaline pH and high lithium chloride concentrations. This data is in agreement with previous literature on *S. cerevisiae*[63], *C. albicans*[25,64] and *A. nidulans*[65] suggesting the participation of Snf7 in the RIM101 signaling cascade. The RIM family includes a sensor protein (RIM21p) and a catalytic complex (RIM20p in association with RIM13p) capable of inducing the proteolytic activation of RIM101p. The lack of Snf7 has been correlated with inability to activate the RIM101 transcription factor independently of the presence of RIM20p and RIM13p[25,35,64]. In fact, the active form of Rim101p supposedly modulates the expression of

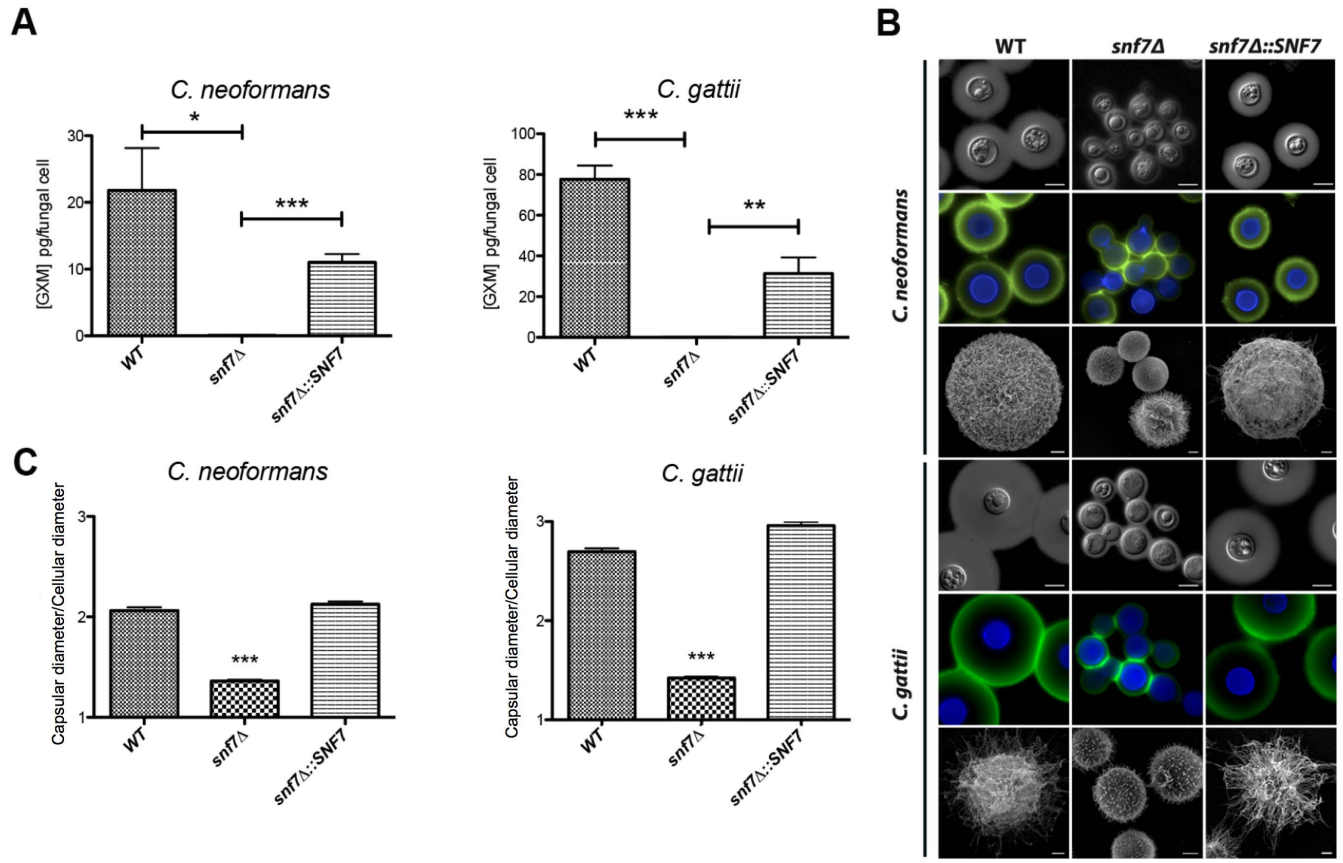

Figure 5 | Surface architecture and GXM release are affected by *SNF7* deletion. (A). Determination of GXM in *C. neoformans* and *C. gattii* culture supernatants. Asterisks denote statistically significant differences (**, $p < 0.005$; ***, $p < 0.001$) between the values obtained for the mutant strains and those obtained for wild type (WT) and complemented (*snf7Δ::SNF7*) cells. (B). Microscopic analysis of WT, *snf7Δ* and *snf7Δ::SNF7* strains of *C. neoformans* and *C. gattii*. India ink counterstaining and immunostaining (upper and middle panels, respectively) revealed that *SNF7* disruption profoundly affects capsule formation. GXM and chitin are stained in green and blue respectively (middle panels). Scale bars represent 5 μm. Scanning electron microscopy of the *C. neoformans* and *C. gattii* strains (Lower panels). Scale bar represents 1 μm. (C). Quantification of capsular dimensions based on *in silico* measurements of the results illustrated in B (***, $p < 0.001$).

several genes involved in the adaptation to different environments[66] and its own expression, which is in agreement with the reduction of *RIM101* mRNA observed in our study.

O'Meara and collaborators have recently shown that Rim101p is also essential for capsule enlargement in *C. neoformans*[35]. Although a *rim101Δ* mutant had normal GXM secretion, several genes involved in cell wall-biosynthesis were affected by *RIM101* deletion, which was likely related to a hypocapsular phenotype[35]. The mutant retained virulence in a murine intranasal infection model, suggesting that secretion of GXM could sufficiently impact host cells in favor of the pathogenic process[35]. The results obtained in our study are in agreement with this supposition. It is noteworthy, however, that the *SNF7* disruption mutants generated in this work additionally had reduced capsules and low efficacy to melanize, which likely renders these cells more susceptible to the antimicrobial arsenal produced by the host. Future studies on how *SNF7* and *RIM101* impact immunomodulation are necessary for a broader understanding on how these cellular pathways interfere with the pathogenic process.

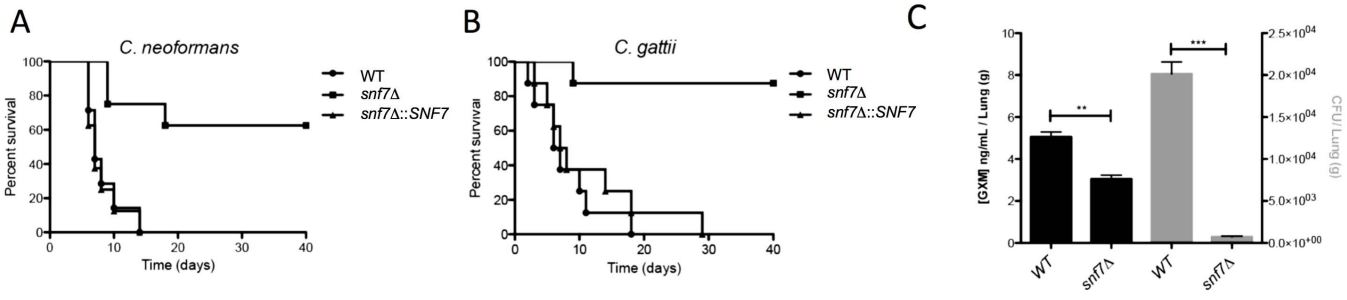

Figure 6 | Cryptococcal virulence is affected by *SNF7* disruption. Mortality rates of mice lethally infected with wild type (WT), mutant (*snf7Δ*) and complemented (*snf7Δ::SNF7*) strains of *C. neoformans* (A) and *C. gattii* (B) were monitored daily. *SNF7* deletion was associated with a non-virulent phenotype in both cryptococcal species. Determination of GXM concentration (black bars) and lung CFU counts (grey bars) in the lungs of mice infected with wild type (CN-WT) and mutant (CN-*snf7Δ*) cells (C) revealed defective polysaccharide production and reduced survival of the mutant (**, $p = 0.0017$; ***, $p < 0.0001$).

Table 1 | List of primers used to construct mutant (*snf7Δ*) and complemented (*snf7Δ::SNF7*) strains of *C. neoformans* and *C. gattii*

Primer name	Sequence (5′- 3′)	Purpose
CnSNF75F	GGGACCACTTTGTACAAGAAAGCTGGGTAATCTTTCACGATGTTGTTTC	Disruption construct for *SNF7*, 5′ flank
CnSNF75R	GGGGACAAGTTTGTACAAAAAAGCAGGCTATTGATACTTATGTCTCGACTA	Disruption construct for *SNF7*, 5′ flank
CnSNF73F	GGGGACCACTTTGTACAAGAAAGCTGGGTAATCTTTCACGATGTTGTTTC	Disruption construct for *SNF7*, 3′ flank
CnSNF73R	AAAAATTACCCTGTTATCCCTTAACCATTGACGAAACCACCGT	Disruption construct for *SNF7*, 3′ flank
CnSNF7compF	CAGATATCCATCACACTGGCGGCCCGTATGGCAATTTCTCATCC	Amplification of *SNF7* for complementation
CnSNF7compR	ACTCACTATAGGGCGAATTGGGCCCCCAATGACACCTGTGCCA	Amplification of *SNF7* for complementation
CnRTSNF7F	GGGACCACTTTGTACAAGAAAGCTGGGTAATCTTTCACGATGTTGTTTC	Amplification of *SNF7* for RT-PCR
CnRTSNF7R	GCGCCAACAGTTATTGATGCT	Amplification of *SNF7* for RT-PCR
CgSNF75F	AAAATAGGGATAACAGGGTAATGATCCTGCGTGGAATGAACAA	Disruption construct for *SNF7*, 5′ flank
CgSNF75R	GGGGACAAGTTTGTACAAAAAAGCAGGCTATCACATCTAATCGAATCGCTTTC	Disruption construct for *SNF7*, 5′ flank
CgSNF73F	GGGGACCACTTTGTACAAGAAAGCTGGGTAGTGTCGATGCTACAATGGACA	Disruption construct for *SNF7*, 3′ flank
CgSNF73R	AAAAATTACCCTGTTATCCCTAGAGGTGGGTTGCTAACCGTAG	Disruption construct for *SNF7*, 3′ flank
CgSNF7compF	CAAGGACAGTGACAACTTGAGG	Amplification of *SNF7* for complementation
CgSNF7compR	GTCTCCCCAAGTGGTGGTATG	Amplification of *SNF7* for complementation
CgRTSNF7F	GGCACACGAGAACGAACTTG	Amplification of *SNF7* for RT-PCR
CgRTSNF7R	GCTCCCTGATCTTGTCCATTG	Amplification of *SNF7* for RT-PCR
CnRIM101F	CGGGCACAAGAAGAGAGAAC	Amplification of *RIM101* for Real time
CnRIM101R	GAGTAAAGAGGCGGCAAATC	Amplification of *RIM101* for Real time
CnRIM20F	CCACTCCTCTTCCTTCTTTCG	Amplification of *RIM20* for Real time
CnRIM20R	TCTCCACCCAATCTTTCCTC	Amplification of *RIM20* for Real time
CgRIM101F	TCCCCTTTCTACCTCAGTTTC	Amplification of *RIM101* for Real time
CgRIM101R	AGCACCAGCATTTCCTTTTG	Amplification of *RIM101* for Real time
CgRIM20F	CAACTCCCCTTCCCTCTTTC	Amplification of *RIM20* for Real time
CgRIM20R	GCCTCTACCCAATCTTTCCTC	Amplification of *RIM20* for Real time
CnRTACTF	CCTTCTACGTCTCTATCCAG	Amplification of *ACT1* for RT-PCR
CnRTACTR	TTTCAAGCTGAGAAGACTGG	Amplification of *ACT1* for RT-PCR

Our observations support the notion that Snf7 expression regulates virulence in both *C. neoformans* and *C. gattii* by reducing polysaccharide and melanin traffic. These results further support the observation that unconventional secretion is essential for cryptococcal pathogenesis[18,58,67] and strongly suggests the occurrence of still obscure mechanisms of exportation of molecules of a non-protein nature in Eukaryotes.

Methods

Fungal strains, plasmids and media. The *C. neoformans* strain H99 (serotype A) and the *C. gattii* strain R265 (serotype B) were the recipients for construction of the mutant strains. Cells were maintained in YPD medium (yeast extract 1%, peptone 2%, glucose 2% and 1.5% agar). To evaluate the effects of Cu^{2+} deprivation on *C. neoformans* and *C. gattii*, cells were grown in 10 mL of YPD broth previous to a further cultivation in 100 mL of Yeast Nitrogen Base broth (YNB) (Becton, Dickinson and Company, Sparks, USA) for 24 hours at 37°C. The cells (5×10^7 cells.mL^{-1}) were then transferred to 50 mL of limited Cu^{2+} medium (LCM) and of Cu^{2+}-replete medium (LCM + Cu) for 12 hours at 37°C with shaking (200 rpm). LCM is identical to a previously described low iron medium (LIM)[68], except for supplementation with 100 μM bathocuproine disulphonate (BCS) (Sigma Chemical Co., Saint Louis, USA) and 100 μM FeHEDTA (Sigma Chemical Co., Saint Louis, USA). LCM + Cu was prepared based on the composition described for iron-replete medium (LIM + Fe)[68,69]. YPD plates with nourseothricin (100 μg/mL) were used to select *C. neoformans SNF7* deletion transformants (CN-*snf7Δ*). YPD plates with hygromycin (200 μg/mL) were used to select *C. neoformans SNF7* complementation transformants (CN-*snf7Δ*::*SNF7*). For *C. gattii*, YPD plates supplemented with hygromycin (200 μg/mL) were used to select *the SNF7* deletion transformants (CG-*snf7Δ*). YPD plates with supplemented nourseothricin (100 μg/mL) were used to select complemented transformants (CG-*snf7Δ*::*SNF7*). Plasmid pJAF15[70] was the source of a hygromycin resistance cassette and pAI4[71] was the source of a nourseothricin resistance cassette. Plasmids were maintained in *Escherichia coli* grown at 37°C for 18 hours in LB broth or agar supplemented with 50 μg/mL of kanamycin.

In silico analysis of C. neoformans and C. gattii SNF7 orthologs. The *C. neoformans* putative *SNF7* gene sequence (Broad Institute accession number CNAG_01583.2) was identified by a BLAST search in the *C. neoformans* var. *grubii* strain H99 genomic database at the Broad Institute database by using the *SNF7* sequence of *C. gattii* (Broad Institute accession number CNBG_3856). The putative amino acid sequences of Snf7 functional homologs in *Saccharomyces cerevisiae* (NCBI accession number P39929.1), *Candida albicans* (NCBI accession number EEQ43071.1), *Aspergillus nidulans* (Broad Institute accession number ANID_04240), *Paracoccidioides brasiliensis* (Broad Institute accession number PAAG_07890.1), *Schizosaccharomyces pombe* (NCBI accession number Q9P7F7), *Neurospora crassa* (Broad Institute accession number NCU01282.5), *Magnaporthe oryzae* (NCBI accession number EHA47375.1), *Arabidopsis thaliana* (NCBI accession number AEE85595.1), *Oryza sativa* (NCBI accession number AAT85290.1), *C. neoformans* (Broad Institute accession number CNAG_01583.2) *and C. gattii* (Broad Institute accession number CNBG_3856) were aligned using Clustal X2[72]. Phylogenetic analysis was performed using Mega5 applying the neighbor-joining method[73]. Tree architecture was inferred from 1,000 bootstraps.

Disruption and complementation of *SNF7*. Delsgate methodology[74–76] was used to construct the *snf7Δ* mutant strains. For the *C. neoformans* mutant, pDONRNAT vector was constructed as previously described[76]. The 5′ and 3′ *SNF7* flanks (~700 bp) were PCR amplified and gel purified using the Illustra GFX PCR DNA and gel band purification kit (GE Healthcare, Fairfield, USA). pDONRNAT (~300 ng) plus 5′ and 3′ PCR products (~30 ng of each) were submitted to BP clonase reaction, according to manufacturer's instructions (Invitrogen, Carlsbad, USA). This reaction mixture was transformed into *Escherichia coli* OmniMAX 2-T1[77]. The deletion construct was linearized by I-SceI enzymatic digestion and submitted to biolistic transformation[78] in *C. neoformans* (H99 strain). The possible *snf7Δ* mutant colonies were screened by PCR, and the deletion was confirmed by Southern blot analysis and reverse transcription-PCR (RT-PCR). For complementation of the *SNF7* mutant, a genomic PCR fragment containing a wild type *C. neoformans SNF7* gene was cloned into the SmaI site of pJAF15 plasmid. Biolistic transformation was performed to introduce the resultant vector into *snf7Δ* mutant strain. Genomic insertion was confirmed by Southern blot and RT-PCR.

The generation of the *C. gattii* mutant and complemented strains was performed as described above for *C. neoformans* with some modifications. For the mutant strain, a hygromicin resistance cassette was used to construct pDONRHYG, which was transformed into *E. coli* TG2 cells. The mutant strains were screened and confirmed as described above. For complementation, a genomic PCR fragment containing the wild-type *C. gattii SNF7* gene was cloned into the SmaI site of the pAI4 plasmid. Genomic insertion was confirmed via Southern blot and RT-PCR.

Primers used to construct and confirm mutant and complemented strains are listed in Table 1.

Phenotypic assays. For spot assays, wild type *C. neoformans* and *C. gattii* (CN-WT and CG-WT), CN-*snf7Δ* and CG-*snf7Δ* mutants and complemented (CN-

snf7Δ::*SNF7* and CG-*snf7Δ*::*SNF7*) strains were cultivated in YPD medium and serially diluted[75]. Diluted cells were spotted in LCM agar, LCM + Cu agar and 150 mM $LiCl_2$[64] (Sigma, St. Louis, MO). Melanin production was visualized in cells spotted on Niger seed agar plates and on defined media containing 1 mM of L-DOPA[79,80]. For capsule analysis, WT, *snf7Δ* and complemented strains of *C. neoformans* and *C. gattii* (5×10^6 cells/mL) were incubated using six well culture plates in DMEM (Invitrogen, Carlsbad, CA) at 37°C and 5% CO_2 for 48 hours. Capsule measurements were performed as previously described[76]. Staining of surface components (chitin and GXM) was performed as described elsewhere[81]. Briefly, fungal cells were fixed in 4% paraformaldehyde (Sigma, St. Louis, MO) for 1 hour followed by a incubation with phosphate-buffered saline (PBS) supplemented with 1% bovine serum albumin (Sigma, St. Louis, MO). Cell structures were then stained using calcofluor white (25 μM) (Sigma, St. Louis, MO) and 18B7 anti GXM monoclonal antibody (1 μg/mL) (kindly provided by Dr. Arturo Casadevall) followed by anti murine IgG Alexa Fluor 488 conjugated (Invitrogen, Carlsbad, CA). Images were acquired using an Axyoplan 2 microscope (Carl Zeiss, Germany). Cell surface structures were also observed by scanning electron microscopy (SEM) as described elsewhere[67]. Analysis of extracellular GXM was performed according to the method described by Casadevall and colleagues[82], with minor modifications[83]. Phospholipase activity was determined by using egg yolk agar[84,85]. Approximately 10^7 cells of WT, *snf7Δ* and complemented strains of both *C. neoformans* and *C. gattii* were spotted onto the center of petri dishes containing egg yolk agar, and incubated at 30°C. After 4 days, the phospholipase activity (*Pz value*) was determined as described by Price and colleagues[84]. To test growth in alkaline pH, YPD medium was buffered with 150 mM HEPES to pH 7, 7.5, 8, 8.5 and 9 with NaOH. Cultures were serially diluted in 96-well microtiter plates containing a pH-tested medium. After incubation at 30°C for 24 hours, absorbance measurements (OD_{600}) were performed using a ELx80 Absorbance Microplate Reader (BioTek, Winooski, VT) and analyzed using GraphPad Prism software. Urease activity was evaluated as described by Kwon-Chung and colleagues[86]. The measurements (OD_{560}) in urea broth were done at 2, 4 and 24 hours interval. All phenotypic assays were performed in triplicate.

Real time quantitative reverse transcription PCR (RT-qPCR) analysis. Cultures of WT, *snf7Δ* and *snf7Δ*::*SNF7* strains of *C. neoformans* and *C. gattii* were grown overnight in YPD medium at 30 °C with shaking. RNA extraction and cDNA synthesis were performed as previously described[75] for all strains in this study. The Applied Biosystems 7500 real-time PCR System (Life Technologies, Carlsbad, CA) was used for real time PCRs and the PCR cycling conditions as well as melting curve and relative expression determination were performed as described[75]. The experiments were performed using two biological samples and each cDNA sample was analyzed in triplicate with each primer pair. Actin cDNA levels were used to normalize each set of PCR experiments. The primer sequences used are listed in the Table 1.

***In vivo* assays.** Mice were intraperitoneally anesthetized with 100 mg/kg ketamine and 16 mg/kg xylazine, followed by intranasal infection[5] with WT, *snf7Δ* and complemented strains of *C. neoformans* and *C. gattii*. For each strain tested, eight female BALB/c mice (approximately 5 weeks old) were used. Fungal cells were first grown in YPD medium at 30°C, 200 RPM shaking, during 20 hours. The cells were washed twice and suspended in PBS solution. The infections were performed by inoculation of 10^7 yeast cells suspended in 50 μL PBS per animal. Infected mice were monitored daily. Mantel-Cox tests were performed using GraphPad Prism software. For CFU determination and *in vivo* GXM analysis, groups of 3 female BALB/c mice (approximately 5 weeks old) were inoculated intratracheally with 10^7 cells of CN-WT and CN-*snf4Δ* strains. After 6 days animals were sacrificed and the lungs were removed and macerated in 5 mL YPD at 4°C. Macerates were clarified by centrifugation and supernatants were quantitatively assessed for the presence of GXM by ELISA as described previously[82]. Alternatively, 5 μL of the macerates were plated on YPD solid medium for further incubation at 37°C (48 h) and CFU counting.

Ethics Statement. The Universidade Federal do Rio Grande do Sul Ethics Committee for Use of Animals (CEUA - protocol number 19801) approved the use of animals in the present work, which were cared for according to the Brazilian National Council for Animal Experimentation Control (CONCEA) and Brazilian College of Animal Experimentation (COBEA) guidelines. Mice were kept in filtered top ventilated cages with food and water *ad libitum*. Groups of a maximum number of four mice were kept in each cage. All efforts to minimize animal suffering and to reduce the number of animals used were made. Animals were observed twice daily for any signals of suffering and/or for mortality during 40 days.

Statistical analysis. Statistical comparisons were performed with the Graphpad 5.0 software. Paired comparisons between different groups were performed using the Student's t test. Survival curves were statistically analyzed using the Mantel-Cox test.

1. Park, B. J. *et al.* Estimation of the current global burden of cryptococcal meningitis among persons living with HIV/AIDS. *AIDS* **23**, 525–30 (2009).
2. Chayakulkeeree, M. & Perfect, J. R. Cryptococcosis. *Infect Dis Clin North Am* **20**, 507–44, v-vi (2006).
3. Byrnes, E. J. 3rd, Bartlett, K. H., Perfect, J. R. & Heitman, J. *Cryptococcus gattii*: an emerging fungal pathogen infecting humans and animals. *Microbes Infect* **13**, 895–907 (2011).
4. Steenbergen, J. N. & Casadevall, A. The origin and maintenance of virulence for the human pathogenic fungus *Cryptococcus neoformans*. *Microbes Infect* **5**, 667–75 (2003).
5. Cox, G. M., Mukherjee, J., Cole, G. T., Casadevall, A. & Perfect, J. R. Urease as a virulence factor in experimental cryptococcosis. *Infect Immun* **68**, 443–8 (2000).
6. Nickel, W. & Rabouille, C. Mechanisms of regulated unconventional protein secretion. *Nat Rev Mol Cell Biol* **10**, 148–55 (2009).
7. Schekman, R. Charting the secretory pathway in a simple eukaryote. *Mol Biol Cell* **21**, 3781–4 (2010).
8. Rodrigues, M. L., Franzen, A. J., Nimrichter, L. & Miranda, K. Vesicular mechanisms of traffic of fungal molecules to the extracellular space. *Curr Opin Microbiol* **16**, 414–20 (2013).
9. Casadevall, A., Nosanchuk, J. D., Williamson, P. & Rodrigues, M. L. Vesicular transport across the fungal cell wall. *Trends Microbiol* **17**, 158–62 (2009).
10. Vecchiarelli, A. Immunoregulation by capsular components of *Cryptococcus neoformans*. *Med Mycol* **38**, 407–17 (2000).
11. Bose, I., Reese, A. J., Ory, J. J., Janbon, G. & Doering, T. L. A yeast under cover: the capsule of *Cryptococcus neoformans*. *Eukaryot Cell* **2**, 655–63 (2003).
12. Garcia-Rodas, R. & Zaragoza, O. Catch me if you can: phagocytosis and killing avoidance by *Cryptococcus neoformans*. *FEMS Immunol Med Microbiol* **64**, 147–61 (2012).
13. Zaragoza, O. *et al.* The capsule of the fungal pathogen *Cryptococcus neoformans*. *Adv Appl Microbiol* **68**, 133–216 (2009).
14. Villena, S. N. *et al.* Capsular polysaccharides galactoxylomannan and glucuronoxylomannan from *Cryptococcus neoformans* induce macrophage apoptosis mediated by Fas ligand. *Cell Microbiol* **10**, 1274–85 (2008).
15. Rodrigues, M. L. *et al.* Vesicular polysaccharide export in *Cryptococcus neoformans* is a eukaryotic solution to the problem of fungal trans-cell wall transport. *Eukaryot Cell* **6**, 48–59 (2007).
16. Rodrigues, M. L. & Djordjevic, J. T. Unravelling secretion in *Cryptococcus neoformans*: more than one way to skin a cat. *Mycopathologia* **173**, 407–18 (2012).
17. Rodrigues, M. L. *et al.* Extracellular vesicles produced by *Cryptococcus neoformans* contain protein components associated with virulence. *Eukaryot Cell* **7**, 58–67 (2008).
18. Oliveira, D., Rizzo, J., Joffe, L., Godinho, R. & Rodrigues, M. Where Do They Come from and Where Do They Go: Candidates for Regulating Extracellular Vesicle Formation in Fungi. *Int J Mol Sci* **14**, 9581–9603 (2013).
19. Weiss, P., Huppert, S. & Kolling, R. Analysis of the dual function of the ESCRT-III protein Snf7 in endocytic trafficking and in gene expression. *Biochem J* **424**, 89–97 (2009).
20. Shestakova, A. *et al.* Assembly of the AAA ATPase Vps4 on ESCRT-III. *Mol Biol Cell* **21**, 1059–71 (2010).
21. Peck, J. W., Bowden, E. T. & Burbelo, P. D. Structure and function of human Vps20 and Snf7 proteins. *Biochem J* **377**, 693–700 (2004).
22. Michelet, X., Djeddi, A. & Legouis, R. Developmental and cellular functions of the ESCRT machinery in pluricellular organisms. *Biol Cell* **102**, 191–202 (2010).
23. Babst, M. MVB vesicle formation: ESCRT-dependent, ESCRT-independent and everything in between. *Curr Opin Cell Biol* **23**, 452–7 (2011).
24. Maeda, T. The signaling mechanism of ambient pH sensing and adaptation in yeast and fungi. *FEBS J* **279**, 1407–13 (2012).
25. Wolf, J. M. & Davis, D. A. Mutational analysis of *Candida albicans* SNF7 reveals genetically separable Rim101 and ESCRT functions and demonstrates divergence in bro1-domain protein interactions. *Genetics* **184**, 673–94 (2010).
26. Chen, Y. *et al.* The *Cryptococcus neoformans* Transcriptome at the Site of Human Meningitis. *MBio* **5**, e01087–13 (2014).
27. Rittershaus, P. C. *et al.* Glucosylceramide synthase is an essential regulator of pathogenicity of *Cryptococcus neoformans*. *J Clin Invest* **116**, 1651–9 (2006).
28. Chun, C. D. & Madhani, H. D. Ctr2 links copper homeostasis to polysaccharide capsule formation and phagocytosis inhibition in the human fungal pathogen *Cryptococcus neoformans*. *PLoS One* **5**, e12503 (2010).
29. Silva, F. D. *et al.* Effects of microplusin, a copper-chelating antimicrobial peptide, against *Cryptococcus neoformans*. *FEMS Microbiol Lett* **324**, 64–72 (2011).
30. Kullas, A. L., Li, M. & Davis, D. A. Snf7p, a component of the ESCRT-III protein complex, is an upstream member of the RIM101 pathway in *Candida albicans*. *Eukaryot Cell* **3**, 1609–18 (2004).
31. Wolf, J. M. & Davis, D. A. Mutational analysis of Candida albicans SNF7 reveals genetically separable Rim101 and ESCRT functions and demonstrates divergence in bro1-domain protein interactions. *Genetics* **184**, 673–94 (2010).
32. Xu, W., Smith, F. J., Jr., Subaran, R. & Mitchell, A. P. Multivesicular body-ESCRT components function in pH response regulation in Saccharomyces cerevisiae and Candida albicans. *Mol Biol Cell* **15**, 5528–37 (2004).
33. Bowers, K. *et al.* Protein-protein interactions of ESCRT complexes in the yeast *Saccharomyces cerevisiae*. *Traffic* **5**, 194–210 (2004).
34. Lamb, T. M., Xu, W., Diamond, A. & Mitchell, A. P. Alkaline response genes of *Saccharomyces cerevisiae* and their relationship to the RIM101 pathway. *J Biol Chem* **276**, 1850–6 (2001).
35. O'Meara, T. R. *et al.* Interaction of *Cryptococcus neoformans* Rim101 and protein kinase A regulates capsule. *PLoS Pathog* **6**, e1000776 (2010).
36. Chen, S. C. *et al.* Identification of extracellular phospholipase B, lysophospholipase, and acyltransferase produced by *Cryptococcus neoformans*. *Infect Immun* **65**, 405–11 (1997).

37. Cox, G. M. *et al.* Extracellular phospholipase activity is a virulence factor for *Cryptococcus neoformans*. *Mol Microbiol* **39**, 166–75 (2001).
38. Park, M., Do, E. & Jung, W. H. Lipolytic enzymes involved in the virulence of human pathogenic fungi. *Mycobiology* **41**, 67–72 (2013).
39. Kronstad, J. W. *et al.* Expanding fungal pathogenesis: *Cryptococcus* breaks out of the opportunistic box. *Nat Rev Microbiol* **9**, 193–203 (2011).
40. O'Meara, T. R. & Alspaugh, J. A. The *Cryptococcus neoformans* capsule: a sword and a shield. *Clin Microbiol Rev* **25**, 387–408 (2012).
41. Rodrigues, M. L. *et al.* Vesicular transport systems in fungi. *Future Microbiol* **6**, 1371–81 (2011).
42. Noverr, M. C., Cox, G. M., Perfect, J. R. & Huffnagle, G. B. Role of PLB1 in pulmonary inflammation and cryptococcal eicosanoid production. *Infect Immun* **71**, 1538–47 (2003).
43. Santangelo, R. *et al.* Role of extracellular phospholipases and mononuclear phagocytes in dissemination of cryptococcosis in a murine model. *Infect Immun* **72**, 2229–39 (2004).
44. Wright, L. C. *et al.* Cryptococcal phospholipases: a novel lysophospholipase discovered in the pathogenic fungus Cryptococcus gattii. *Biochem J* **384**, 377–84 (2004).
45. Eisenman, H. C., Frases, S., Nicola, A. M., Rodrigues, M. L. & Casadevall, A. Vesicle-associated melanization in *Cryptococcus neoformans*. *Microbiology* **155**, 3860–7 (2009).
46. Turner, K. M., Wright, L. C., Sorrell, T. C. & Djordjevic, J. T. N-linked glycosylation sites affect secretion of cryptococcal phospholipase B1, irrespective of glycosylphosphatidylinositol anchoring. *Biochim Biophys Acta* **1760**, 1569–79 (2006).
47. Hanson, P. I. & Cashikar, A. Multivesicular body morphogenesis. *Annu Rev Cell Dev Biol* **28**, 337–62 (2012).
48. Panepinto, J. *et al.* Sec6-dependent sorting of fungal extracellular exosomes and laccase of *Cryptococcus neoformans*. *Mol Microbiol* **71**, 1165–76 (2009).
49. Yoneda, A. & Doering, T. L. A eukaryotic capsular polysaccharide is synthesized intracellularly and secreted via exocytosis. *Mol Biol Cell* **17**, 5131–40 (2006).
50. Hu, G. *et al.* *Cryptococcus neoformans* requires the ESCRT protein Vps23 for iron acquisition from heme, for capsule formation, and for virulence. *Infect Immun* **81**, 292–302 (2013).
51. Oliveira, D. L. *et al.* Characterization of yeast extracellular vesicles: evidence for the participation of different pathways of cellular traffic in vesicle biogenesis. *PLoS One* **5**, e11113 (2010).
52. Albuquerque, P. C. *et al.* Vesicular transport in *Histoplasma capsulatum*: an effective mechanism for trans-cell wall transfer of proteins and lipids in ascomycetes. *Cell Microbiol* **10**, 1695–710 (2008).
53. Duran, J. M., Anjard, C., Stefan, C., Loomis, W. F. & Malhotra, V. Unconventional secretion of Acb1 is mediated by autophagosomes. *J Cell Biol* **188**, 527–36 (2010).
54. Manjithaya, R., Anjard, C., Loomis, W. F. & Subramani, S. Unconventional secretion of *Pichia pastoris* Acb1 is dependent on GRASP protein, peroxisomal functions, and autophagosome formation. *J Cell Biol* **188**, 537–46 (2010).
55. Oliveira, D. L. *et al.* Biogenesis of extracellular vesicles in yeast: Many questions with few answers. *Commun Integr Biol* **3**, 533–5 (2010).
56. Burgoyne, T. *et al.* Expression of OA1 limits the fusion of a subset of MVBs with lysosomes - a mechanism potentially involved in the initial biogenesis of melanosomes. *J Cell Sci* **126**, 5143–52 (2013).
57. Kim, S. J. & Brandizzi, F. The Plant Secretory Pathway: An Essential Factory for Building the Plant Cell Wall. *Plant Cell Physiol* **55**, 687–693 (2014).
58. Kmetzsch, L. *et al.* Role for Golgi reassembly and stacking protein (GRASP) in polysaccharide secretion and fungal virulence. *Mol Microbiol* **81**, 206–18 (2011).
59. Hu, G. & Kronstad, J. W. A putative P-type ATPase, Apt1, is involved in stress tolerance and virulence in *Cryptococcus neoformans*. *Eukaryot Cell* **9**, 74–83 (2010).
60. Rizzo, J. *et al.* Role of the Apt1 Protein in Polysaccharide Secretion by Cryptococcus neoformans. *Eukaryot Cell* **13**, 715–26 (2014).
61. Nosanchuk, J. D. & Casadevall, A. Impact of melanin on microbial virulence and clinical resistance to antimicrobial compounds. *Antimicrob Agents Chemother* **50**, 3519–28 (2006).
62. Tu, J., Vallier, L. G. & Carlson, M. Molecular and genetic analysis of the SNF7 gene in *Saccharomyces cerevisiae*. *Genetics* **135**, 17–23 (1993).
63. Xu, W., Smith, F. J., Subaran, R. & Mitchell, A. P. Multivesicular body-ESCRT components function in pH response regulation in Saccharomyces cerevisiae and Candida albicans. *Mol Biol Cell* **15**, 5528–37 (2004).
64. Kullas, A. L., Li, M. & Davis, D. A. Snf7p, a component of the ESCRT-III protein complex, is an upstream member of the RIM101 pathway in Candida albicans. *Eukaryot Cell* **3**, 1609–18 (2004).
65. Tilburn, J., Sánchez-Ferrero, J. C., Reoyo, E., Arst, H. N. & Peñalva, M. A. Mutational analysis of the pH signal transduction component PalC of *Aspergillus nidulans* supports distant similarity to BRO1 domain family members. *Genetics* **171**, 393–401 (2005).
66. Peñalva, M. A. & Arst, H. N. Regulation of gene expression by ambient pH in filamentous fungi and yeasts. *Microbiol Mol Biol Rev* **66**, 426–46, table of contents (2002).
67. Rizzo, J. *et al.* Role of the Apt1 protein in polysaccharide secretion by *Cryptococcus neoformans*. *Eukaryot Cell* **13**, 715–726 (2014).
68. Jacobson, E. S., Goodner, A. P. & Nyhus, K. J. Ferrous iron uptake in *Cryptococcus neoformans*. *Infect Immun* **66**, 4169–75 (1998).
69. Lian, T. *et al.* Iron-regulated transcription and capsule formation in the fungal pathogen *Cryptococcus neoformans*. *Mol Microbiol* **55**, 1452–72 (2005).
70. Fraser, J. A., Subaran, R. L., Nichols, C. B. & Heitman, J. Recapitulation of the sexual cycle of the primary fungal pathogen *Cryptococcus neoformans* var. *gattii*: implications for an outbreak on Vancouver Island, Canada. *Eukaryot Cell* **2**, 1036–45 (2003).
71. Idnurm, A., Reedy, J. L., Nussbaum, J. C. & Heitman, J. *Cryptococcus neoformans* virulence gene discovery through insertional mutagenesis. *Eukaryot Cell* **3**, 420–9 (2004).
72. Larkin, M. A. *et al.* Clustal W and Clustal X version 2.0. *Bioinformatics* **23**, 2947–8 (2007).
73. Tamura, K. *et al.* MEGA5: molecular evolutionary genetics analysis using maximum likelihood, evolutionary distance, and maximum parsimony methods. *Mol Biol Evol* **28**, 2731–9 (2011).
74. García-Pedrajas, M. D. *et al.* DelsGate, a robust and rapid gene deletion construction method. *Fungal Genet Biol* **45**, 379–88 (2008).
75. Kmetzsch, L. *et al.* The vacuolar Ca(2)(+) exchanger Vcx1 is involved in calcineurin-dependent Ca(2)(+) tolerance and virulence in *Cryptococcus neoformans*. in *Eukaryot Cell,* Vol. **9**, 1798–805 (2010).
76. Kmetzsch, L. *et al.* The GATA-type transcriptional activator Gat1 regulates nitrogen uptake and metabolism in the human pathogen *Cryptococcus neoformans*. *Fungal Genet Biol* **48**, 192–9 (2011).
77. Schneider Rde, O. *et al.* Zap1 Regulates Zinc Homeostasis and Modulates Virulence in *Cryptococcus gattii*. *PLoS One* **7**, e43773 (2012).
78. Toffaletti, D. L., Rude, T. H., Johnston, S. A., Durack, D. T. & Perfect, J. R. Gene transfer in *Cryptococcus neoformans* by use of biolistic delivery of DNA. *J Bacteriol* **175**, 1405–11 (1993).
79. Kmetzsch, L. *et al.* Role for Golgi reassembly and stacking protein (GRASP) in polysaccharide secretion and fungal virulence. *Mol Microbiol* **81**, 206–18 (2011).
80. Baker, L. G., Specht, C. A., Donlin, M. J. & Lodge, J. K. Chitosan, the deacetylated form of chitin, is necessary for cell wall integrity in *Cryptococcus neoformans*. *Eukaryot Cell* **6**, 855–67 (2007).
81. Rodrigues, M. L., Alvarez, M., Fonseca, F. L. & Casadevall, A. Binding of the wheat germ lectin to *Cryptococcus neoformans* suggests an association of chitinlike structures with yeast budding and capsular glucuronoxylomannan. *Eukaryot Cell* **7**, 602–9 (2008).
82. Casadevall, A., Mukherjee, J. & Scharff, M. D. Monoclonal antibody based ELISAs for cryptococcal polysaccharide. *J Immunol Methods* **154**, 27–35 (1992).
83. Fonseca, F. L. *et al.* Structural and functional properties of the *Trichosporon asahi*i glucuronoxylomannan. *Fungal Genet Biol* **46**, 496–505 (2009).
84. Price, M. F., Wilkinson, I. D. & Gentry, L. O. Plate method for detection of phospholipase activity in *Candida albicans*. *Sabouraudia* **20**, 7–14 (1982).
85. Chen, S. C., Muller, M., Zhou, J. Z., Wright, L. C. & Sorrell, T. C. Phospholipase activity in *Cryptococcus neoformans*: a new virulence factor? *J Infect Dis* **175**, 414–20 (1997).
86. Kwon-Chung, K. J., Wickes, B. L., Booth, J. L., Vishniac, H. S. & Bennett, J. E. Urease inhibition by EDTA in the two varieties of *Cryptococcus neoformans*. *Infect Immun* **55**, 1751–4 (1987).
87. Selvig, K. & Alspaugh, J. A. pH Response Pathways in Fungi: Adapting to Host-derived and Environmental Signals. *Mycobiology* **39**, 249–56 (2011).
88. Livak, K. J. & Schmittgen, T. D. Analysis of relative gene expression data using real-time quantitative PCR and the 2(-Delta Delta C(T)) Method. *Methods* **25**, 402–8 (2001).

Acknowledgments

We thank Fernanda L. Fonseca for help with microscopy tests and Debora L. Oliveira for help with in vivo experimentation. We are also grateful to Drs. Josh Nosanchuk, Maurizio Del Poeta and Leonardo Nimrichter for helpful suggestions. This work was supported by grants from the Brazilian agencies CNPq, CAPES, FAPERJ and MCT/FINEP/Rede GENOPROT (grant number 01.07.0552.00). JC received a scholarship (grant number 201227/2009-6) for a 6 months stay at The Scripps Research Institute, USA. The authors also acknowledge support from the Instituto Nacional de Ciência e Tecnologia de Inovação em Doenças Negligenciadas (INCT-IDN).

Author contributions

R.M.C.G., J.C., M.H.V. and M.L.R. wrote the main manuscript text; R.M.C.G. and J.C. prepared all figures; R.M.C.G., J.C., G.S.A., S.F. and L.K. conducted the experiments. R.M.C.G., J.C., G.S.A., S.F., L.K., C.C.S., A.S., M.H.V. and M.L.R. analyzed the data and reviewed the manuscript.

Additional information

Competing financial interests: The authors declare no competing financial interests.

How to cite this article: da C. Godinho, R.M. *et al.* The vacuolar-sorting protein Snf7 is required for export of virulence determinants in members of the *Cryptococcus neoformans* complex. *Sci. Rep.* **4**, 6198; DOI:10.1038/srep06198 (2014).